Molecular Dynamics-Based Analysis of Cavity Distribution in GeO_2 Glass: A Novel Computational Method

N V Hong[1], P T Dung[1], N. H Anh[2], M T Lan[1]

[1]*Faculty of Engineering Physics, Hanoi University of Science and Technology, Hanoi 100000, Vietnam*

[2]*Colorado School of Mines, Golden, CO 80401, USA*

GeO_2 glass is a material of significant interest due to its applications in optics and microelectronics. Despite its widespread use, the presence and distribution of cavities (voids) within the glass structure remain inadequately understood. This study presents a novel method for calculating and analyzing the distribution of cavities in GeO_2 glass using molecular dynamics simulation data. The approach involves: (1) constructing an atomistic model of GeO_2 glass via molecular dynamics simulations; (2) detecting and quantifying cavities within the glass, including their spatial locations and sizes; and (3) performing statistical analysis to derive the cavity size distribution function. The findings demonstrate that this method effectively determines the size and spatial distribution of cavities in GeO_2 glass. Enhanced understanding of cavity distribution can inform strategies to optimize the optical and structural properties of GeO_2 glass. This cavity calculation method offers a valuable tool for probing the nanoscale architecture of glass materials.

1. Introduction

Amorphous materials such as germanium oxide (GeO_2) and silica (SiO_2) glasses are of considerable interest due to their unique optical, electronic, and mechanical properties [1-3]. These properties are intimately related to the atomic-scale structure and morphology of the glassy network, particularly the presence and distribution of cavities or voids within the material [4-11].

Cavities in glass structures can profoundly influence the material's physical and chemical characteristics. For instance, the size, shape, and connectivity of cavities can affect ion and molecule diffusion rates, alter the efficiency of adsorption processes and catalytic reactions, as well as modify optical transmission and scattering properties [7-15]. Consequently, developing accurate methods to characterize the distribution of cavities in glass networks is essential for understanding and engineering the desired properties of these materials.

While conventional experimental techniques such as positron annihilation spectroscopy, small-angle X-ray scattering, and nitrogen adsorption provide insights into the presence and size of cavities in glasses [7, 15-18], they are limited in their ability to resolve the detailed spatial distribution and connectivity of cavities at the nanoscale. In this study, we propose a data mining approach based on molecular dynamics (MD) simulations to systematically investigate the cavity distribution in GeO_2 glass. MD simulations offer a detailed atomistic representation of the glass structure, which can be utilized to develop a comprehensive cavity analysis methodology. By integrating advanced data processing and statistical analysis techniques, we aim to extract valuable insights into cavity characteristics and their relation to the overall glass network structure. The primary objectives of this study are: (1) to establish a robust computational framework for detecting and quantifying cavities in GeO_2 glass using MD data; (2) to analyze the size distribution, spatial

distribution, and connectivity of the cavities; and (3) to demonstrate the utility of this cavity analysis approach in understanding the structure-property relationships in glass materials.

2. Calculation method

In this study, we analyzed the cavity distribution in GeO_2 glass using a computational approach grounded in molecular dynamics (MD) simulation data. The key steps of the calculation method are outlined below:

MD Model Construction: A GeO_2 glass model was generated using classical MD simulations, employing the Oeffner-Elliott (OE) interatomic potential. The simulation box comprised 5,499 atoms (1,833 Ge and 3,666 O atoms) with periodic boundary conditions. The system was equilibrated at 5000 K and then gradually cooled to 300 K to obtain the final amorphous glass structure [4, 12, 19-22].

Monte Carlo-Based Cavity Volume Calculation: To quantify the cavity volume fraction and its distribution within the glass network, a Monte Carlo approach was utilized. A total of 1,500,000 random points were uniformly distributed within the MD simulation box. For each point, a determination was made as to whether it resided within a cavity (i.e., a region unoccupied by any atoms). The proportion of points located within cavities provided an estimate of the cavity volume fraction [22-27].

Cavity Detection and Size Distribution Analysis: The spatial distribution and sizes of the cavities were determined using the DBSCAN (Density-Based Spatial Clustering of Applications with Noise) algorithm [23-24]. This algorithm clusters data points that are closely located based on a distance metric and the minimum number of points required to form a cluster. In this study, DBSCAN was applied to the set of random points identified as being within cavities. The algorithm enabled the identification of individual cavities and their respective volumes, allowing for the construction of a cavity size distribution function that offers insights into the statistical characteristics of the cavity network in GeO_2 glass. All calculations and data analyses were performed using custom Python scripts, leveraging scientific computing libraries such as NumPy, SciPy, and scikit-learn.

DBSCAN Parameters: The key parameters for the DBSCAN algorithm are epsilon (eps) and *min_samples*. Epsilon defines the maximum distance between two points for them to be considered as part of the same neighborhood, thereby determining the cluster density. *Min_samples* specifies the minimum number of points required to form a dense region, distinguishing between core points (points with at least min_samples neighbors within epsilon) and border points (points with fewer than *min_samples* neighbors within epsilon) [24, 28].

Visualizing Cavity Distribution: To visualize the distribution of cavities in 3D space, we employed a technique of filling the cavity volumes with small spheres. This approach provides a clear visualization of the cavities' spatial distribution.

3. Results and discussion

To optimize the key parameters (*epsilon* and *min_samples)* we have calculated and displayed the nearest neighbor distance graph as in figure 1.

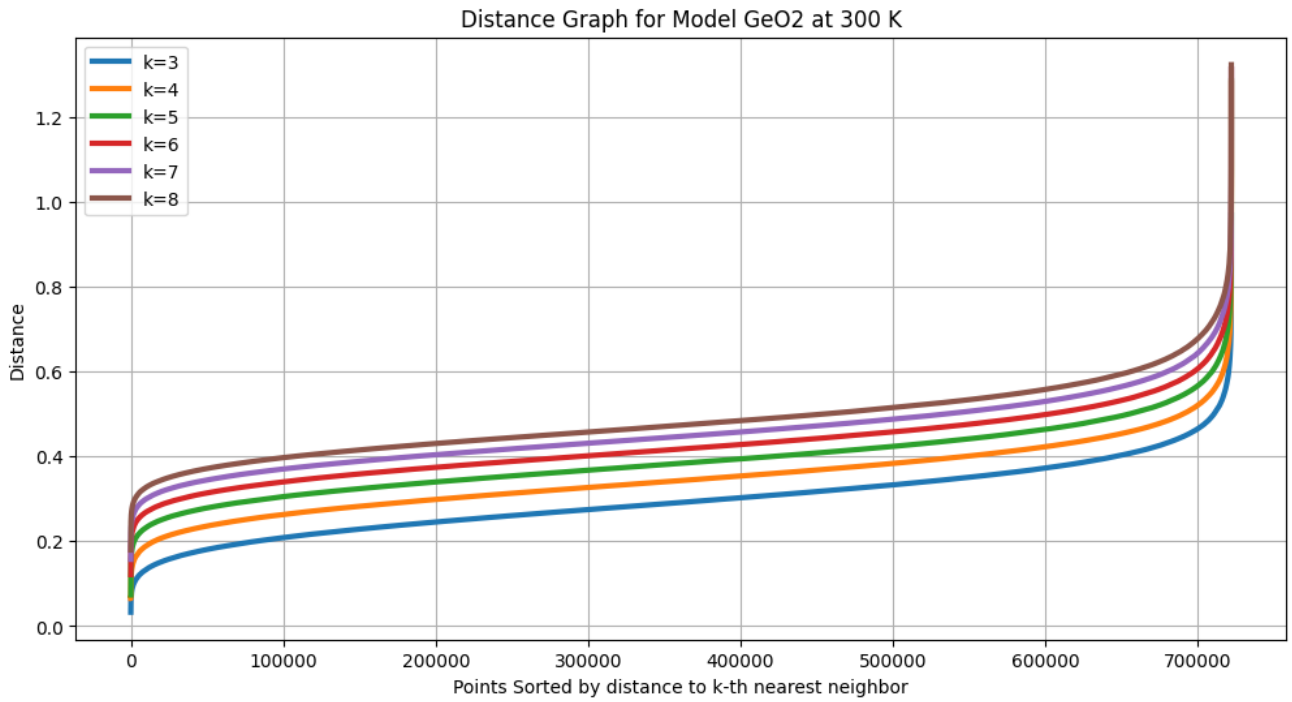

The figure shows that the *min_samples* of 3-8 corresponds to a distance of 0.4-0.7Å. We choose the *min-samples* to be 2*d = 6, where d=3 is the number of dimensions. We choose the eps = 0.41 Å, this value ensures that the total volume of cavities is about 75-80 % the free volume of the model.

Table 1. Cavities volume distribution and volume fraction of large cavities, where V_M, V_F and V_{TC} are model volume, free volume and total cavities volume, respectively.

Cavity type	Total cavities	Top 10	Top 50	Top 100	Top 200	Top 500
V (Å^3)	32077	2941	7859	10812	13894	18194
V/V_M(%)	38%	3.5%	9.4%	12.9%	16.6%	21.7%
V/V_F(%)	79.5%	7.3%	19.5%	26.8%	34.4%	45.1%
V/V_{TC}(%)	100.0%	9.2%	24.5%	33.7%	43.3%	56.7%
Note: V_M= of 83,861 Å^3, V_F=40,358 Å^3, the total number of cavities in model =573755.						

The GeO_2 model consists of 5,499 atoms in a cubic box with a volume of 83,861 Å^3. The free volume of the model is 40,358 Å^3, see table 1. Figure 2 shows the distribution of top 10 cavities in 3D space. The cavities (voids) within the GeO_2 glass structure are represented by clusters of colored spheres, each color corresponding to a different cavity or void. On the right side of the figure, there is a list of individual cavities (labeled as voids) with their corresponding volumes in cubic angstroms (Å³).

The distribution shows a variety of cavity sizes and shapes, with some cavities forming extended, interconnected structures, while others appear as isolated clusters. The DBSCAN algorithm has successfully identified and clustered cavities based on the spatial proximity of points within the MD simulation box. The visualization emphasizes the spatial relationships and connectivity between cavities, highlighting regions where voids are densely packed or more isolated. It can be seen that the largest cavity with volume of 457 $Å^3$ (corresponding to over 1% total free volume of the model) is formed due to interconnection of many cavities. The next top 2-9 cavities have the volume of 352, 319, 300, 285, 269, 268, 251, 226 and 214 $Å^3$, respectively. Total volume of top 10 cavities is 2,941 $Å^3$ (about 7.3 % the total free volume, corresponding to 3.5 % the model volume), see table 1. Figure 3 shows the spatial distribution and corresponding size of the top 11-50 cavities. Their volume is from about 80 to 200 $Å^3$. Total volume of the top 50 cavities is 7,859 $Å^3$ (about 19.5% the total free volume of model).

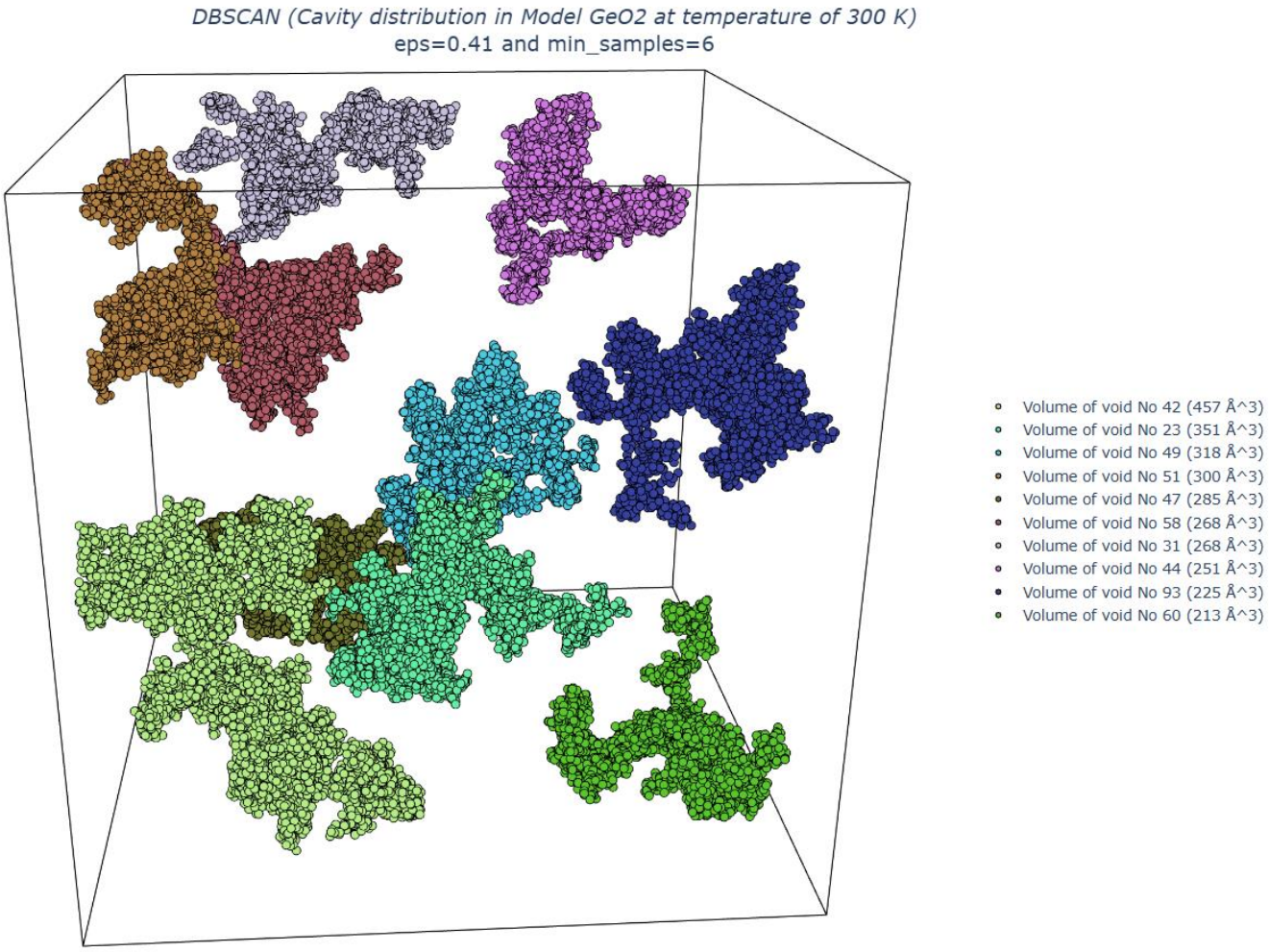

Fig. 2 *The size and spatial distribution of the top 10 cavities in model.*

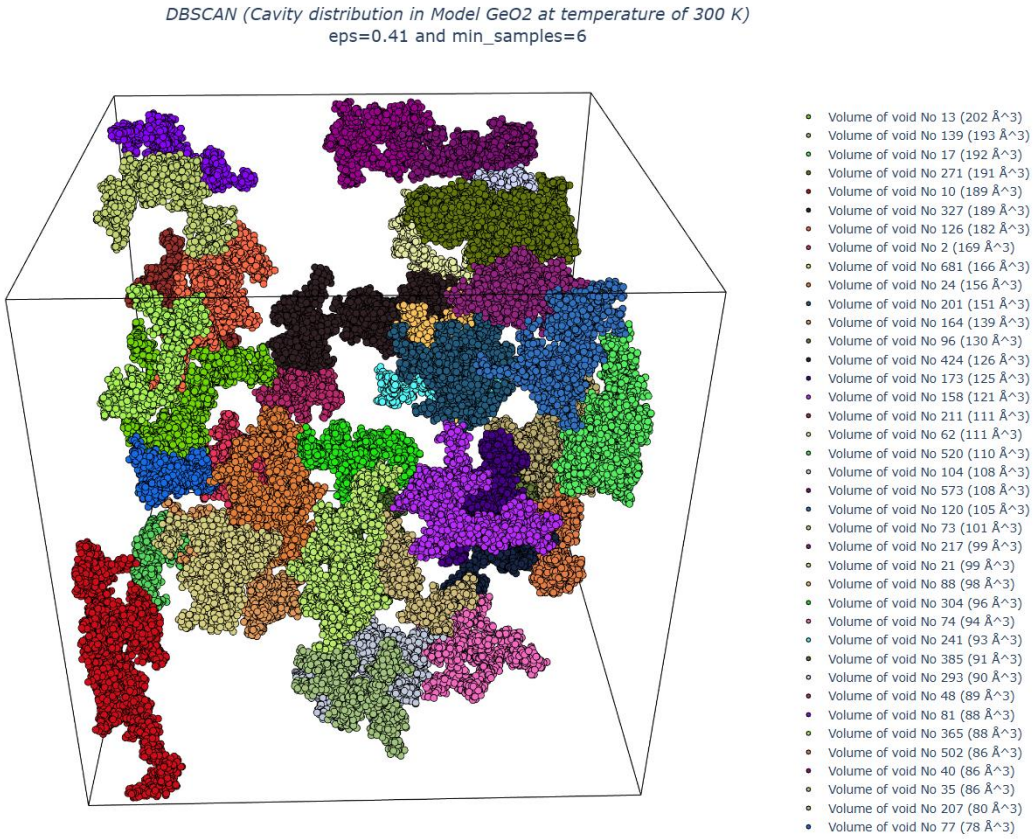

Fig. 3 *The distribution of the top 11-50 cavities in the model.*

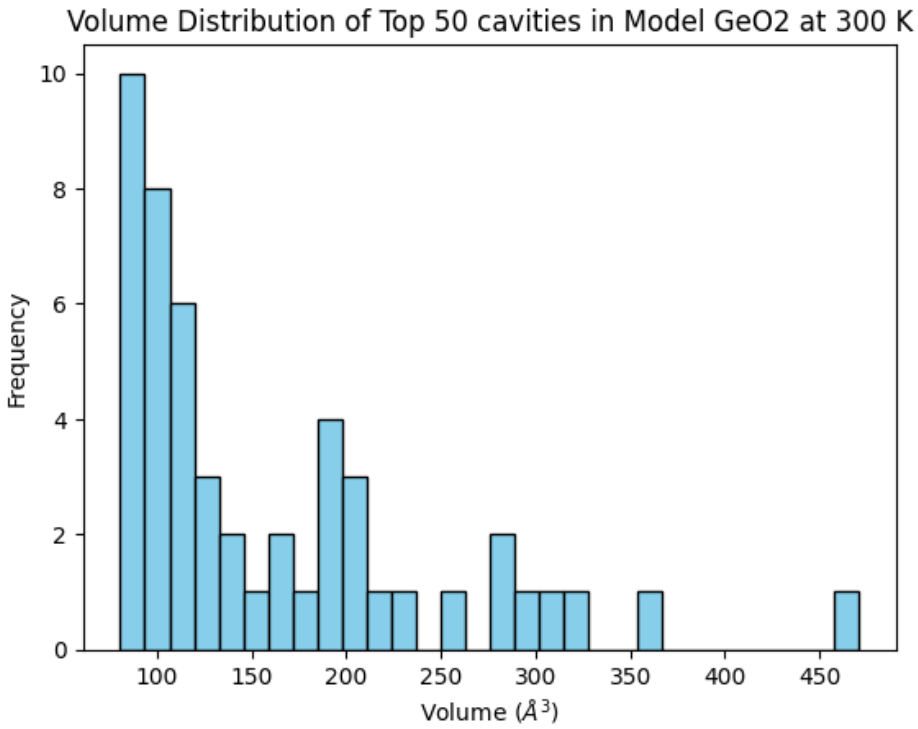

Fig.4. *The volume distribution of top 50 cavities in the model*

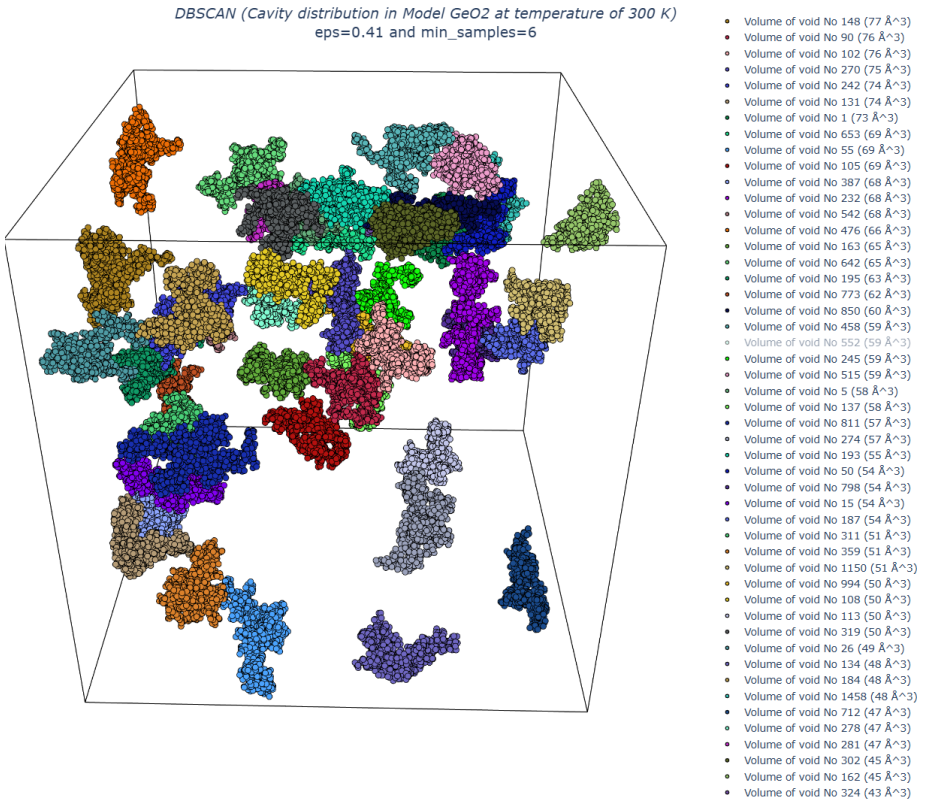

Fig.5. *Volume distribution of the top 51-100 cavities in the model*

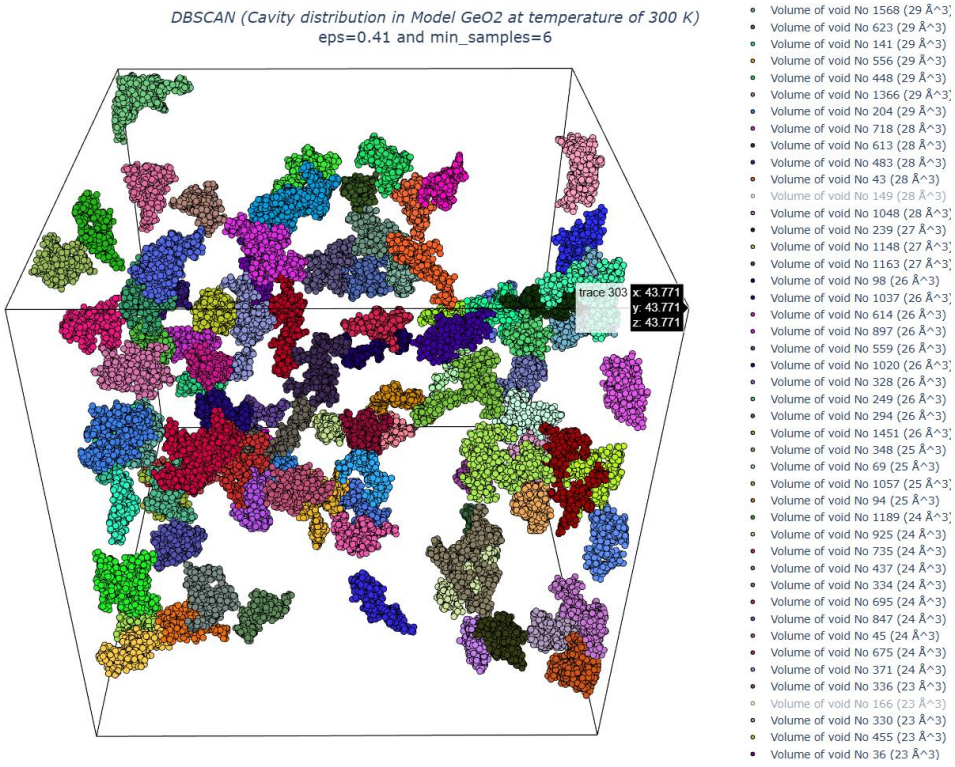

Fig.6. *Volume distribution of top 101-200 cavities in the model*

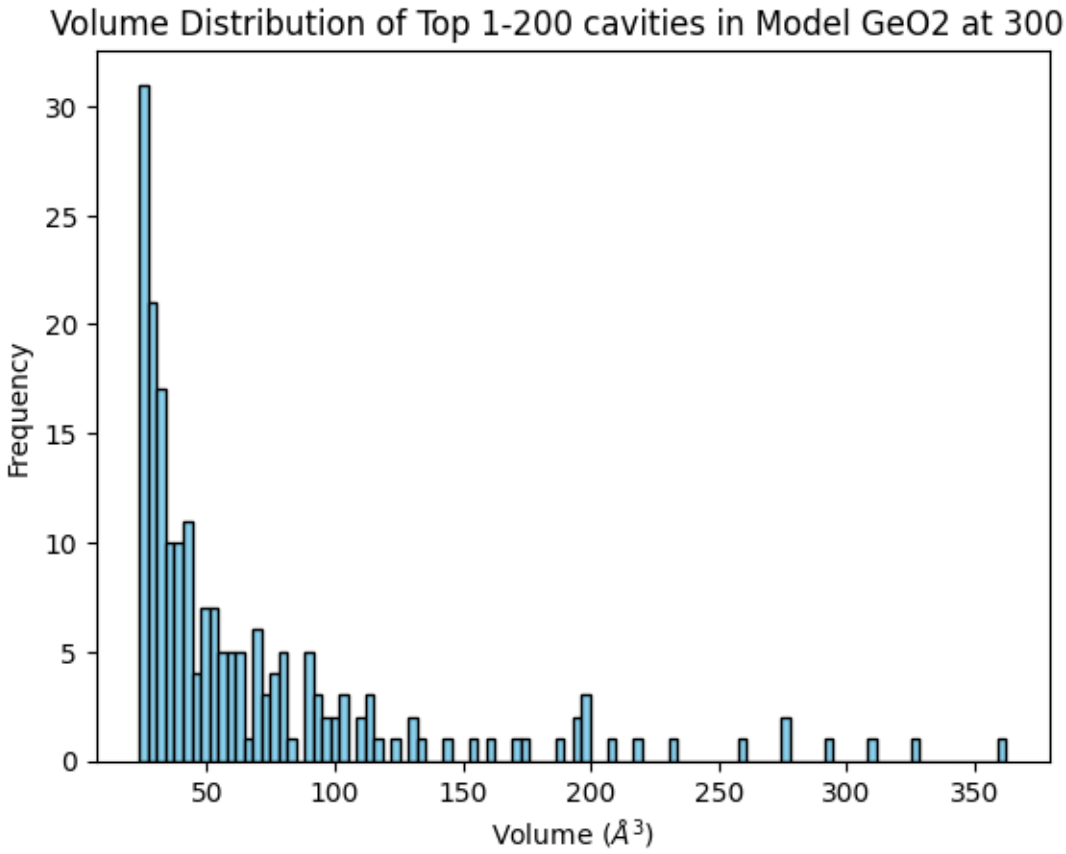

Fig.7. *Volume distribution of top 200 cavities in the model*

Figure 4 shows the volume distribution statistics of the largest cavities (Top 50). It can be seen that most of cavities (in top 50) have volume of around between 100 and 200 Å³. The model has about ten cavities, with each one having a volume of more than 200 Å³, see figure 2.

Figure 5 shows the volume distribution of cavities in the top 51-100 cavities, volume is from 43 to 77 Å³. Meanwhile, the volume distribution of cavities in top 101-200 is from 23 to 42 Å³, see figure 6.

Figure 7 displays the frequency of cavities based on their volume, measured in cubic angstroms (Å³). Most cavities have relatively small volumes, with the highest frequency occurring in the range of approximately 20-30 Å³. The frequency of cavities decreases as the volume increases, indicating that smaller cavities are more common in the glass structure. A steep decline is observed after the 30-40 Å³ range, with very few cavities exceeding 100 Å³ in volume. A small number of cavities have volumes between 200 Å³ and 350 Å³, indicating the presence of a few larger cavities, although these are rare. This distribution suggests that in the GeO_2 glass structure at 300 K, smaller cavities are dominant, while larger cavities are much less frequent. The overall trend is typical for amorphous materials where smaller voids or cavities are more common due to the random nature of the atomic arrangement.

This visualization and the associated data provide insights into the nanoscale structure of GeO_2 glass, particularly the distribution and connectivity of cavities. Such information is crucial for understanding how the presence and distribution of voids can affect the material's macroscopic properties, such as optical transmission, diffusion, and mechanical strength.

4. Conclusion

In this study, we employed molecular dynamics simulations and DBSCAN clustering to analyze the distribution and characteristics of cavities within GeO_2 glass. Our results reveal significant insights into the spatial arrangement and volume distribution of these voids. By optimizing the key parameters, we determined that a minimum of 6 samples and an epsilon value of 0.41 Å effectively captured the majority of cavity structures, ensuring that the total volume of cavities approximates 75-80% of the free volume within the model.

The analysis identified a broad spectrum of cavity sizes and configurations. Specifically, the largest cavity, with a volume of 457 $Å^3$, significantly contributes to the overall free volume, while the top ten cavities alone account for approximately 7.3% of the total free volume. The volume distribution indicates that smaller cavities are far more prevalent than larger ones, with the majority of cavities falling within the 20-30 $Å^3$ range. This trend is consistent with the general characteristics of amorphous materials, where smaller voids are more common due to the disordered nature of the atomic structure.

Our findings are illustrated by detailed visualizations (Figures 2-7), which showcase the spatial distribution of cavities and highlight regions of high and low void density. This information is instrumental in understanding how the structural characteristics of GeO_2 glass, particularly the distribution and size of cavities, can influence its macroscopic properties.

References:

[1] Benjamin Walker et al., Electronic structure and optical properties of amorphous GeO2 in comparison to amorphous SiO2, J Non-Cryst Solids 428, 176–183 (2015).

[2] Shigeki Sakaguchi and Shin-ichi Todoroki, "Optical properties of GeO2 glass and optical fibers," Appl. Opt. 36, 6809-6814 (1997)

[3] Nobuaki Terakado, Keiji Tanaka, The structure and optical properties of GeO2–GeS2 glasses, Journal of Non-Crystalline Solids, Vol. 354, **18**, pp 1992-1999 (2008).

[4] Yohei Onodera, Topological analyses of structure of glassy materials toward extraction of order hidden in disordered structure, J. Ceramic Society of Japan 130, **8** 627-638 (2022) (cavity)

[5] Taylor, J.M., Fai, T.G., Virga, E.G. et al. Cavity Volume and Free Energy in Many-Body Systems. J Nonlinear Sci 31, 87 (2021). https://doi.org/10.1007/s00332-021-09744-y.

[6] Zhen Zhang, Simona Ispas, and Walter Kob, Fracture of silicate glasses: Microcavities and correlations between atomic-level properties, Phys. Rev. Materials 6, 085601 – Published 15 August 2022.

[7] Abdelal N, Donaldson SL. Comparison of methods for the characterization of voids in glass fiber composites. *Journal of Composite Materials*. 2018;52(4):487-501. doi:10.1177/0021998317710083

[8] Gelb, Lev D. AU - Gubbins, K. E., Pore Size Distributions in Porous Glasses: A Computer Simulation Study, Langmuir 1999, 15, **2**, 305–308 (1998): doi: 10.1021/la9808418

[9] Tomohiro Hashimoto et al. Void formation in glasses, *New J. Phys.* **9** 253 *(* 2007)

[10] Setsuro Ito, Taketoshi Taniguchi, Madoka Ono, Ken Uemura, Network and void structures for glasses with a higher resistance to crack formation, Journal of Non-Crystalline Solids, Vol. 358, 24, 3453-3458, (2012)

[11] Adrian C. Wright, Density fluctuations in vitreous SiO2 and GeO2, Phys. Chem. Glasses: Eur. J. Glass Sci. Technol. B, 60, **2**, 33–48, (2019)

[12] Ting Li, Shiping Huang, Jiqin Zhu, The structure and void analysis of pressure-induced amorphous GeO2: Molecular dynamics simulation, Chemical Physics Letters, Vol. 471, Issues 4–6, 253-257 (2009)

[13] Nadezhda M. Korobatova, Olga N. Koroleva, Effect of the SiO2/GeO2 ratio in the Na2O-B2O3-SiO2-GeO2 system on the characteristics of porous glasses, Materialia, Vol. 27, 101669, (2023)

[14] G. Kartopu et. al., Structural and optical properties of porous nanocrystalline Ge, J. Appl. Phys. 103, 113518 (2008)

[15] Nigel J. Shevchik, William Paul, Voids in amorphous semiconductors, J of Non-Cryst. Solids,

Vol. 16, Issue 1, Pages 55-71 (1974).

[16] Elsherif, Ahmed Gamal Attallah Abdelmaksoud, Study of the pore systems of metal-organic frameworks, mesoporous silica, and low-k dielectric layers by means of positron annihilation spectroscopy, PhDThesis, Universitäts- und Landesbibliothek Sachsen-Anhalt, (2018)

[17] Mikhail R. Baklanov, Konstantin P. Mogilnikov, Alexey S. Vishnevskiy, Challenges in porosity characterization of thin films: Cross-evaluation of different techniques, J. Vac. Sci. Technol. A 41, 050802 (2023)

[18] Zhichong Yu, Liang Tang, Nattapol Ma, Satoshi Horike, Wenqian Chen, Recent progress of amorphous and glassy coordination polymers, Coordination Chemistry Reviews, Vol. 469, (2022)

[19] Nguyen Van Hong, Correlation between structure and dynamics of liquid GeO2 under compression, Chemical Physics Letters Vol. 845, **16**, 141307 (2024)

[20] Nguyen Mai Anh, Nguyen Thi Thu Trang, To Thi Nguyet, Nguyen Van Linh, Nguyen Van Hong, Densification mechanism of GeO2 glass under high pressure: Insight from analyzation and visualization of molecular dynamics data, Computational Materials Science, Vol. 177, 109597 (2020)

[21] Tran Thuy Duong, Toshiaki Iitaka, Pham Khac Hung, Nguyen Van Hong, The first peak splitting of the Ge-Ge pair RDF in the correlation to network structure of GeO2 under compression, J Non-Cryst. Solids, Vol. 459, PP. 103-110, (2017)

[22] Hung, P., Hong, N. Simulation study of polymorphism and diffusion anomaly for SiO_2 and GeO_2 liquid. *Eur. Phys. J. B* **71**, 105–110 (2009). https://doi.org/10.1140/epjb/e2009-00276-2.

[23] Zeina Abu-Aisheh, Romain Raveaux, Jean-Yves Ramel, Efficient k-nearest neighbors search in graph space, Pattern Recognition Letters, Volume 134, 2020, Pages 77-86.

[24] Alireza Latifi-Pakdehi, Negin Daneshpour, DBHC: A DBSCAN-based hierarchical clustering algorithm, *Data & Knowledge Engineering, Volume 135, 2021, 101922*,

[25] Yewang Chen et al., KNN-BLOCK DBSCAN: Fast Clustering for Large-Scale Data, *IEEE Transactions on Systems, Man, and Cybernetics: Systems (Vol. 51, **6,** 3939 - 3953 (2021)*

[26] Santilli, Tullio, X.P.S. studies of differences in contamination behaviour of amorphous and crystalline germanium, *Masters Thesis (1978). https://doi.org/10.26190/unsworks/7926*

[27] Amanda J. Parker and Amanda S. Barnard, Selecting Appropriate Clustering Methods for Materials Science Applications of Machine Learning, *Advanced Theory and Simulations, **Volume2, (12**), 1900145 (2019)*

[28] D. Deng, DBSCAN Clustering Algorithm Based on Density, *7th International Forum on Electrical Engineering and Automation (IFEEA), Hefei, China, 2020, pp. 949-953, (2020). doi: 10.1109/IFEEA51475.2020.00199.*